

1
2
3
4
5
6
7
8
9
10
11
12
13
14
15
16
17
18
19
20
21
22
23
24
25

Neighbor predation linked to natural competence fosters the transfer of large genomic regions in *Vibrio cholerae*

Noémie Matthey¹, Sandrine Stutzmann¹, Candice Stoudmann¹, Nicolas Guex²,
Christian Iseli² and Melanie Blokesch^{1*}

¹Laboratory of Molecular Microbiology, Global Health Institute, School of Life Sciences, Ecole Polytechnique Fédérale de Lausanne (Swiss Federal Institute of Technology Lausanne; EPFL), Lausanne, Switzerland; ²Swiss Institute of Bioinformatics, Lausanne, Switzerland

* *Corresponding author:*
Melanie Blokesch
Ecole Polytechnique Fédérale de Lausanne (EPFL)
Station 19, UPBLO
CH-1015 Lausanne, Switzerland
Tel: +41 21 693 0653
Email: melanie.blokesch@epfl.ch

Abbreviations: horizontal gene transfer – HGT; genomic DNA – gDNA; transforming DNA – tDNA; quorum-sensing – QS

Short title: DNA transfer among co-cultured *V. cholerae*

Keywords: DNA uptake, natural competence, transformation, type VI secretion

26 **Abstract**

27 Natural competence for transformation is a primary mode of horizontal gene transfer (HGT).
28 Competent bacteria are able to absorb free DNA from their surroundings and exchange this DNA
29 against pieces of their own genome when sufficiently homologous. And while it is known that
30 transformation contributes to evolution and pathogen emergence in bacteria, there are still
31 questions regarding the general prevalence of non-degraded DNA with sufficient coding capacity.
32 In this context, we previously showed that the naturally competent bacterium *Vibrio cholerae*
33 uses its type VI secretion system (T6SS) to actively acquire DNA from non-kin neighbors under
34 chitin-colonizing conditions. We therefore sought to further explore the role of the T6SS in
35 acquiring DNA, the condition of the DNA released through T6SS-mediated killing versus
36 passive cell lysis, and the extent of the transfers that occur due to these conditions. To do this, we
37 herein measured the frequency and the extent of genetic exchanges in bacterial co-cultures on
38 competence-inducing chitin under various DNA-acquisition conditions. We show that competent
39 *V. cholerae* strains acquire DNA fragments with an average and maximum length exceeding
40 50 kbp and 150 kbp, respectively, and that the T6SS is of prime importance for such HGT events.
41 Collectively, our data support the notion that the environmental lifestyle of *V. cholerae* fosters
42 HGT and that the coding capacity of the exchanged genetic material is sufficient to significantly
43 accelerate bacterial evolution.

44

45 **Significance Statement**

46 DNA shuffled from one organism to another in an inheritable manner is a common feature of
47 prokaryotes. It is a significant mechanism by which bacteria acquire new phenotypes, for
48 example by first absorbing foreign DNA and then recombining it into their genome. In this study,
49 we show the remarkable extent of the exchanged genetic material, frequently exceeding 150
50 genes in a seemingly single transfer event, in *Vibrio cholerae*. We also show that to best preserve

51 its length and quality, bacteria mainly acquire this DNA by killing adjacent, healthy neighbors
52 then immediately absorbing the released DNA before it can be degraded. These new insights into
53 this prey-killing DNA acquisition process shed light on how bacterial species evolve in the wild.

54

55 **Introduction**

56 The causative agent of the diarrheal disease cholera, *Vibrio cholerae*, is responsible for seven
57 major pandemics since 1817, one of which is still ongoing. Due to its ability to rapidly spread in
58 contaminated water, cholera poses a serious world health risk, affecting between 1 and 4 million
59 people and causing 21,000–143,000 deaths per year, especially in poor or underdeveloped
60 countries (1). Many disease-causing bacteria have developed mechanisms for rapidly evolving in
61 response to environmental pressures, and these rapid changes are often responsible for the
62 formation of new serogroups with pandemic potential. One way in which *V. cholerae* acquire
63 new phenotypes is through horizontal gene transfer (HGT), which is the direct movement of
64 DNA from one organism to another. A major mode of HGT is natural competence for
65 transformation in which bacteria are able to absorb free DNA from their surroundings using their
66 competence-induced DNA-uptake complex (2-4). When sufficient homology is present between
67 the incoming DNA and the bacterial genome, the absorbed genetic material can be integrated
68 into the genome via double homologous recombination at the expense of the initial DNA region.
69 As an example of the significant power of this natural competence for gene uptake, we
70 previously witnessed the gain of an ~40 kbp O139-antigen cluster at the expense of the original
71 ~30 kbp O1-antigen cluster through natural transformation (followed by strong selective pressure
72 exerted by antibiotics or phages; (5)), which significantly changed the phenotypes of these
73 bacteria. And while Griffith's experiment in 1928 unambiguously proved that transformation
74 contributes to evolution and pathogen emergence, the general prevalence of non-degraded DNA

75 with sufficient coding capacity has been questioned (6), drawing inquiries as to whether this
76 mode of HGT could be responsible for the major changes causing pandemic strains to emerge.

77 The induction of competence in *V. cholerae* is tightly regulated (recently reviewed by (7)).
78 Briefly, upon growth on the (molted) chitin-rich exoskeletons of zooplankton (8), the most
79 abundant polysaccharide in the aquatic environment and therefore an important carbon source for
80 chitinolytic bacteria (9), the expression pattern of *V. cholerae* is altered (10) to render it naturally
81 competent for genetic transformation (11). Initially, when chitin degradation products are sensed
82 by *V. cholerae*, it produces the regulatory protein TfoX (10-15). This competence activator
83 positively regulates the expression of the major DNA-uptake machinery in the cell (4), providing
84 a direct connection between growth on chitin and competence activation. Apart from TfoX,
85 natural competence and transformation also depend on the master regulator of quorum sensing,
86 HapR, in two ways: i) HapR acts as repressor of *dns*, which encodes an extracellular nuclease
87 that inhibits transformation (16); and ii) HapR together with TfoX co-activates the transcription
88 factor QstR, which further represses *dns* as well as activates several DNA-uptake genes (17, 18).

89 While the chitin-induced DNA-uptake complex of *V. cholerae* is able to absorb DNA from
90 the surrounding (19-23), environmental DNA is often heavily degraded and therefore short in
91 size (24, 25). In addition, free DNA is thought to originate from dead and therefore less fit
92 bacteria, which renders the coding part of such genetic material non-favorable for naturally
93 competent bacteria (26). In line with these arguments, we recently showed that *V. cholerae* does
94 not solely rely on randomly released environmental DNA. Instead, it actively acquires “fresh”
95 DNA from healthy, living bacteria through kin-discriminatory neighbor predation (27), which,
96 conceptually, also occurs in other naturally competent bacteria (28). Neighbor predation in *V.*
97 *cholerae* is accomplished by a contractile injection system known as the type VI secretion
98 system (T6SS) that transports toxic effector proteins into prey (29-32). Intriguingly, the T6SS of
99 pandemic *V. cholerae* is exquisitely co-regulated with its DNA-uptake machinery in a TfoX-,

100 HapR-, and QstR-dependent manner when the bacterium grows on chitin (27, 33, 34), which
101 increases the chances of the competent bacterium to take up freshly released DNA compared to
102 free-floating “unfit” DNA. Notably, this coupling of competence and type VI secretion is also
103 conserved in several non-cholera vibrios (35).

104 In the current study, we determined the extent of the absorbed and chromosomally-integrated
105 prey-derived DNA. Previous studies had scored transformation events in other naturally
106 competent Gram-negative bacteria such as *Haemophilus influenzae*, *Helicobacter pylori*, and
107 *Neisseria meningitidis* (36-38). These former studies, however, relied on the supplementation of
108 large quantities of purified DNA (with up to 50 donor genome equivalents per cell (37)) at the
109 peak of the organism’s competence program (36). Such an approach, however, neither
110 recapitulates the natural onset of competence nor discloses the fate of the DNA that is released
111 from dying cells. Thus, to address these points and to mimic natural settings, we determined the
112 frequency and extent of DNA exchanges under chitin-dependent co-culture conditions of two
113 non-clonal *V. cholerae* strains. We show that the DNA transfer frequency is significantly
114 enhanced in T6SS-positive compared to T6SS-negative strains and that large genomic regions
115 are transferred from the killed prey to the competent acceptor bacterium.

116

117 **Results and Discussion**

118 **The T6SS fosters horizontal co-transfer events encompassing two selective markers**

119 To compare the absorption of T6SS-mediated prey-derived DNA as opposed to environmental
120 DNA (released through, for example, random lysis), we first scored the transformability of
121 T6SS-positive (wild-type [WT] predator) and T6SS-negative (acceptor) *V. cholerae* strains,
122 which would allow us to directly measure the contribution of the T6SS on gene uptake. These
123 two strains were co-cultured with non-kin prey (donor) bacteria that were all derived from the
124 environmental isolate Sa5Y (27, 39-41) and contained two antibiotic resistance genes in their

125 genomes: 1) An *aph* cassette (Kan^R), which was integrated in the *vipA* gene on the small
126 chromosome (chr 2); and 2) a *cat* cassette (Cm^R), which was inserted at variable distances from
127 the *aph* cassette on the same chromosome or, alternatively, on the large chromosome (chr 1). As
128 shown in Figure 1, the WT predator strain efficiently absorbed and integrated the prey-released
129 resistance cassettes (*aph* or *cat*), while the transformation efficiency for the T6SS-defective
130 acceptor strain was significantly reduced (by 97.8% and 99.2% for *aph* and *cat*, respectively)
131 (Fig. 1A). Moreover, comparable frequencies were observed for both selective markers,
132 suggesting that their acquisition does not significantly affect the strains' fitness under non-
133 selective conditions. We tested whether these transfer events were indeed competence-mediated
134 and not based on other modes of HGT using a strain with a competence-related DNA import
135 deficiency in that it lacked the competence protein ComEA that reels external DNA into the
136 periplasm (21). This *comEA*-minus strain was never transformed under these predator-prey co-
137 culture conditions, confirming that the gene transfer did depend entirely on natural competence.

138 Next, we scored the frequencies of transformants that had adopted resistance against both
139 antibiotics, which would show the possibility of two transformation events or the transfer of a
140 large piece of DNA (indicated by the distance between the two genes on the same chromosome).
141 These transformations occurred, as expected, at lower rates compared to single-resistant clones
142 and were mostly below the limit of detection for the T6SS-minus acceptor strain (Fig. 1B).
143 Interestingly, we observed a gradual decrease in the frequencies the further the two resistance
144 genes were apart from each other on the same chromosome, while a sharp drop occurred in the
145 number of recovered transformants when the two resistance genes were carried on the two
146 separate prey chromosomes (Fig. 1B). While the latter scenario unambiguously requires at least
147 two separate DNA-uptake events, the former, in which the resistance markers are carried *in cis*,
148 could reflect a mix between single and multiple DNA absorption and integration events. When
149 purified genomic DNA was instead provided as the transforming material to simplify the

150 experiment and provide measurable results for all conditions, the *in cis* double-resistance
151 acquisition efficiencies reached a comparable range to the *in trans* efficiencies when the two
152 resistance genes were separated by at least 100 kbp. This suggested that the more efficient
153 transformations of less than 100 kbp likely often occurred through a single acquisition (Fig. 1C).
154 Furthermore, the WT predator and T6SS-minus acceptor behaved similarly when purified DNA
155 was provided, which makes sense as the need for active DNA release through neighbor predation
156 was eliminated. Based on these data and the fact that the double-acquisition rates for the T6SS-
157 minus acceptor strain were mostly below the detection limit in the prey scenario, we
158 hypothesized that neighbor predation might foster the transfer of long DNA stretches, which
159 frequently exceeded 50 kbp and therefore carry significant coding capacity.

160

161 **Comparative genomics of pandemic strain A1552 and environmental isolate Sa5Y**

162 To test our hypothesis that the T6SS contributes to the horizontal transfer of large DNA
163 fragments, we used a whole-genome sequencing (WGS) approach to properly outline the
164 transferred DNA regions. To do this using WGS, we first needed to characterize the genomes of
165 both the predator/acceptor (A1552) and the prey/donor (Sa5Y) strains for which long-read
166 PacBio sequencing data and *de novo* assemblies without further analysis were recently
167 announced (41). A1552 is a pandemic O1 El Tor strain (42) belonging to the LAT-1 sublineage
168 of the West-African South American (WASA) lineage of seventh pandemic *V. cholerae* strains
169 (43) (see *SI Appendix* for details) while strain Sa5Y was isolated from the Californian Coast (39,
170 40). To understand their genomic arrangements, we also compared these strains to the reference
171 sequence of *V. cholerae* (O1 El Tor strain N16961; (44)) and a re-sequenced laboratory stock of
172 the latter. Details on the comparative genomics between the three pandemic strains (N16961 (44),
173 the newly sequenced and *de novo*-assembled genome sequence of the laboratory stock of
174 N16961, and A1552) are provided in the *SI Appendix* and as Figure S1-S2. We expected to see

175 significant differences in the pandemic A1552 strain compared to the environmental isolate
176 Sa5Y in terms of the absence/presence of genomic features and single nucleotide polymorphisms
177 (SNPs) in core genes that would allow us to measure HGT events occurring between the strains,
178 and several of these major differences are highlighted here. Indeed, as expected from its non-
179 clinical origin, the environmental isolate lacked several genomic regions, including those that
180 encode major virulence features, namely *Vibrio* pathogenicity islands 1 and 2 (VPI-1, VPI-2),
181 *Vibrio* seventh pandemic islands I and II (VSP-I, VSP-II (45)), the cholera toxin prophage CTX
182 (46), and the WASA-1 element. In addition, the strain's O-antigen cluster differed significantly
183 from the O1-encoding genes of pandemic strain A1552 (Fig. 2). The region that differed the
184 most between both strains was the integron island, which is consistent with the role of this
185 assembly platform in fostering the incorporation of exogenous open reading frames (47). Given
186 these major differences between strain A1552 and Sa5Y and, in addition, an overall SNP
187 frequency of approximately 1 in 55 nucleotides for conserved genes, we concluded that HGT
188 events occurring between these two strains on chitinous surfaces could be precisely scored using
189 short-read sequencing. Apart from this important genomic information, we also noted that the
190 pandemic strains as well as Sa5Y contained previously unrecognized rRNA operons, with nine
191 or ten rRNA clusters in total compared to the initially reported eight (44).

192

193 **Released DNA from T6SS-killed prey leads to the transfer of large genomic regions**

194 As our previous study witnessed gene transfers between *V. cholerae* bacteria (5) though neither
195 scored the full extent of the transferred DNA region nor took T6SS-mediated neighbor predation
196 into consideration, we sought to next determine how much genetic material would be absorbed
197 and integrated by competent *V. cholerae* upon neighbor predation. To do this, we co-cultured the
198 predator (A1552) and prey (Sa5Y) strains on chitinous surfaces for 30 h without any deliberate
199 selection pressure. To be able to afterwards screen for the transfer of at least one gene, we first

200 integrated an *aph* cassette within the *vipA* of strain Sa5Y, which concomitantly deactivated the
201 prey's T6SS, to select kanamycin-resistant transformants of strain A1552. Using this system,
202 resistant transformants of A1552 were selected at an average frequency of 1.8×10^{-4} after the
203 30 h co-culturing on chitin (Fig. S3), and 20 of those transformants were randomly picked for
204 further analysis. After three independent experiments, the whole genome of each of the 60
205 transformants was sequenced, and the reads were mapped to either the predator's or the prey's
206 genome sequence (see *SI Appendix* for detailed bioinformatic analysis). As shown in Figure 3,
207 apart from the common acquisition of the *aph* resistance cassette, the location and the size of the
208 prey-donated genomic region differed significantly between most transformants. Previous
209 estimates of the average length of total acquired DNA were made in experiments using purified
210 donor gDNA and were considered to be ~23 kbp (40). Importantly, we observed in these new
211 experiments that the average length of the total acquired DNA, meaning the DNA surrounding
212 the *aph* cassette plus any transferred regions elsewhere on either of the two chromosomes (Fig.
213 S4), was almost 70 kbp and therefore significantly larger than the previous estimates. Around 15%
214 of all transformants acquired and integrated more than 100 kbp (Fig. 3B), which was previously
215 considered unlikely due to absence of such long DNA fragments in the environment. Consistent
216 with the principle of natural transformation, it should be noted that the new DNA was acquired
217 through double homologous recombination such that it replaced the initial DNA region and the
218 overall genome size did not significantly change. Further analysis indicated that about 50% of
219 the strains experienced a single HGT event around the *aph* cassette, while the others exchanged
220 regions in up to eight different locations on the two chromosomes (Fig. 3C). Finally, we
221 analyzed the length of continuous DNA stretches that were acquired from the prey and observed
222 that those ranged from a few kbp up to 168 kbp (Fig. 3D). Collectively, these data indicate that *V.*
223 *cholerae* can acquire large genomic regions from killed neighbors with an average exchange of
224 more than 50 kbp or ~50 genes. This finding contradicts the notion that natural transformation

225 cannot serve for DNA repair or acquisition of new genetic information due to the insufficient
226 length and coding capacity of the acquired genetic material.

227

228 **Transformation by purified DNA only occurs if correctly timed**

229 To better understand the DNA acquisition and integration potential of naturally competent *V.*
230 *cholerae*, we next compared the data described above, which we refer to from now on as
231 condition ① using experiments varying the aspects of neighbor predation and DNA
232 supplementation (Fig. 4A). First, the acceptor strain was grown in a monoculture immediately
233 supplemented with purified genomic DNA (gDNA) derived from the same donor (prey) strain as
234 described above. Notably, when the gDNA was added at the start of the chitin-dependent culture,
235 no transformants were reproducibly detected from three independent biological experiments,
236 suggesting that free DNA is rapidly degraded under such conditions. This finding is consistent
237 with our previous work in which we demonstrated that *V. cholerae* produces an extracellular and
238 periplasmic nuclease Dns (16, 20) that degrades transforming material. At high cell density
239 (HCD), where competence is induced, *dns* is partially repressed through direct binding of HapR
240 (16, 17), and this repression is reinforced by the transcription factor QstR (17, 18). We therefore
241 concluded that the simultaneous expression of both machineries, concomitantly with a strong
242 repression of *dns*, is a prerequisite for successful DNA transfer. Indeed, such coordinated
243 expression would ensure that T6SS-mediated attacks are exquisitely timed with low nuclease
244 activity so that the prey-released DNA can be efficiently absorbed.

245 As we previously showed that the addition of purified gDNA after ~20–24 h of growth on
246 chitin wasn't prone to degradation by Dns (48), we next choose this time point to probe the DNA
247 acquisition capability using purified DNA (condition ②; Fig. 4A). Doing so led to similar
248 transformation frequencies as those observed for the prey-released DNA caused by T6SS attacks
249 (condition ①; Fig. S3A). WGS of 20 transformants from two biologically independent

250 experiments likewise resulted in similar DNA acquisition patterns with average and maximum
251 DNA acquisitions of 70 kbp and 188 kbp, respectively, and the presence of multiple exchanged
252 regions of varying sizes (Fig. 4 and Fig. S5). While we cannot entirely exclude that the
253 maximum length of individual DNA stretches was biased by the purification step, despite the
254 fact that we chose a method that was designed for chromosomal DNA isolation of 20–150 kbp
255 sized fragments (see methods), our results suggest that the maximum DNA acquisition length of
256 single fragments is probably reached between 100–110 kbp (Fig. S5). Moreover, the comparable
257 acquisition patterns between conditions ① and ② (Fig. 4) imply that the prey-released DNA in
258 condition ① is neither heavily fragmented nor is its accessibility or absorption by the competent
259 acceptor bacterium significantly hindered due to, for example, DNA-binding proteins.

260

261 **Prey-exerted T6SS counter attacks do not change the DNA transfer pattern**

262 Since the *aph* cassette was located within the T6SS sheath protein gene *vipA* in the above
263 experiments, we wondered if this T6SS inactivation biased the DNA transfer efficiency. We
264 therefore repeated the above-described experiments using prey strains that carried the *aph*
265 cassette on the opposite site of chr 2 (within gene VCA0747; condition ③). As shown in Figure
266 S3, similar transformation frequencies were observed independent of the position of the *aph*
267 cassette. Moreover, WGS of 2 x 20 transformants showed similar average and maximum DNA
268 acquisition values (55.7 kbp and 227.4 kbp, respectively; Fig. 4) as well as similar distribution
269 patterns around the resistance marker (Fig. S6). However, while not statistically supported, it
270 appeared as if these conditions were prone to the acquisition of multiple non-connected regions,
271 as transformants with only single/connected exchanges dropped from ~50% (Fig. S4 for
272 condition ①) to around 20% (Fig. S6 for condition ③). Based on this observation, we
273 hypothesized that the now-restored T6SS-mediated killing capacity of the prey led to the
274 additional release of genomic DNA from the predator, which interfered with the uptake of prey-

275 released DNA. To test this idea, we repeated condition ③ (e.g., *aph* within VCA0747) though
276 again inactivated the T6SS of the prey using a non-selected marker (*cat*; condition ④), expecting
277 the results to be similar to those of condition ① if this hypothesis was correct. No statistically
278 significant differences were observed between both conditions (③ and ④) for all tested
279 characteristics including transformation frequency (Fig. S3B), number of exchanges, and
280 separate and collective length (Fig. 4 and Figs. S6-S7), suggesting that predator-released DNA
281 does not interfere with the predator's overall transformability by the prey-released DNA.
282 However, we acknowledge that the technical limitations of the experimental setup did not allow
283 the identification of complete revertants that first acquired and then again lost the *aph* cassette.

284

285 **T6SS-independent prey lysis rarely triggers DNA transfer and results in shorter DNA** 286 **exchanges**

287 We next tested whether T6SS-mediated DNA release impacted the length of the exchanged
288 region, which would support the above speculation that the intimate co-regulation of type VI
289 secretion, nuclease repression, and DNA uptake ensures that freshly released DNA is rapidly
290 absorbed by the predator and is therefore less prone to fragmentation. Such co-regulation would
291 not hold true for T6SS-independent DNA release as a result of random cell lysis, so we tested the
292 transfer efficiency of the *aph* cassette under conditions in which both donor and acceptor strains
293 were T6SS-defective (condition ⑤; Fig. 4 and S8). Under such conditions, the transformation
294 frequency dropped by 99.7% (Fig. S3B), and WGS of 2 x 20 of these rare transformants showed
295 significant differences. Indeed, the average and maximal length of acquired DNA (Fig. 4A) and
296 the number of exchanged regions (Fig. 4B) were significantly different when T6SS+ versus
297 T6SS- acceptor strains were compared, with the latter exchanges never exceeding four events
298 compared to up to 13 events for T6SS-mediated DNA release (Figs. S7 and S8). Based on these

299 data, we conclude that T6SS-mediated DNA acquisition not only increases the transfer efficiency
300 by ~100-fold but also fosters the exchange of multiple DNA stretches of extended lengths.

301

302 **T6SS-mediated DNA exchanges are not limited to the small chromosome**

303 The experiments described above were designed to primarily score the transfer efficiency of
304 DNA fragments localized on chr 2. The rationale behind this approach was a recent population
305 genomic study on *Vibrio cyclitrophicus* that suggested the mobilization of the entire chr 2 and
306 caused the authors to speculate: “how often and by what mechanism are entire chromosomes
307 mobilized?” (49). In the current study, we were unable to experimentally show such large
308 transfer events. We considered four potential reasons for the absence of such large transfers: 1)
309 mild fragmentation of prey-released DNA that excluded fragments above ~200 kb; 2) limited
310 DNA uptake and periplasmic storage capacity of the acceptor strain (20, 21); 3) limited
311 protection of the incoming single-stranded DNA by dedicated proteins (such as Ssb and DprA;
312 (50, 51)); or 4) lethality of larger exchanges due to the presence of multiple toxin/antitoxin
313 modules within the integron island on chr 2 of *V. cholerae* (52). While technical limitations did
314 not allow us to address the first three points, we followed up on the last idea by repeating the
315 above-described experiments using prey strains in which the *aph* cassette was integrated on the
316 large chromosome 1 (inside *lacZ*). We used these to test three (co-)culture conditions in which
317 the prey strain was either T6SS-positive (condition ⑥), T6SS-negative (condition ⑦), or
318 replaced by purified gDNA (condition ⑧; Fig. 4A). As shown in Figure S3, the *aph* cassette was
319 again transferred with high efficiency from the killed prey strain to the acceptor strain. However,
320 comparing conditions ⑥ (co-culture conditions) and ⑧ (prey-derived purified gDNA as
321 transforming material) revealed a small but significant transformation increase (~ 4-fold; Fig.
322 S3A). Based on these data, we speculate that the larger size of chr 1 (~3 Mb) compared to chr 2
323 (~1 Mb) slightly lowers the probability of acquiring the *aph* cassette when released from killed

324 prey. This effect becomes negligible when purified gDNA is provided, most likely due to the
325 size constraints of the purification procedure (max. 150 kb). Consistent with this idea was the
326 finding that purified gDNA from all those prey strains described in this study resulted in the
327 same level of transformation no matter where the selective marker was located (Fig. S3D).

328 Next, we randomly picked 20 transformants from two biologically independent experiments
329 for each of these three experimental conditions (Ⓒ to Ⓔ) and sequenced their genomes (Fig. S9-
330 S11). The analysis of these transformants showed that the average and maximum DNA
331 acquisition values were highly comparable to those described above for DNA exchanges on chr 2
332 (Fig. 4A) and that multiple exchanged regions were likewise observed (Fig. 4B). We therefore
333 conclude that prey-derived transforming DNA can equally modify both chromosomes. Moreover,
334 our data suggest that consecutive stretches of exchanged DNA above ~200 kbp either do not
335 occur or occur at levels below the detection limit of this study, and that this size limitation is not
336 caused by the toxin/antitoxin–module-containing integron island on chr 2.

337

338 **Conclusion**

339 Based on the data presented above, we conclude that T6SS-mediated predation followed by
340 DNA uptake leads to the exchange of large DNA regions that can bring about bacterial evolution.
341 This finding is consistent with the heterogeneous environmental *V. cholerae* populations that
342 were observed in cholera-endemic areas (53). Still, an open question that remains is why
343 pandemic cholera isolates are seemingly clonal in nature (43, 54-56), and we propose two
344 explanations for this. First, sampling strategies might be biased for the selection of the most
345 pathogenic strains and, concomitantly, exclude less virulent variants that have undergone HGT
346 events. Secondly, transformation-inhibiting nucleases similar to Dns (16) have recently spread
347 throughout pandemic *V. cholerae* isolates as part of mobile genetic elements (experimentally
348 shown for VchInd5 (57) and predicted for SXT (58)), which makes these pandemic strains less

349 likely to undergo HGT events. One could also argue that pandemic *V. cholerae* are rarely
350 exposed to competence-inducing chitinous surfaces due to the prevalence of inter-household
351 transmission throughout cholera outbreaks (59). Yet *in vivo*-induced antigen technology (IVIAT)
352 assays showed strong human immune responses against proteins of the DNA-uptake pilus that
353 fosters natural transformation, kin recognition, and chitin colonization (10, 11, 19, 23), which
354 contradicts this idea. Indeed, the major pilin PilA was most frequently identified by IVIAT
355 together with the outer-membrane secretin PilQ (60), which suggests that the bacteria encounter
356 competence-inducing conditions either before entering the human host or after its colonization.
357 The latter option is not, however, supported by *in vivo* expression data from human volunteers
358 (61). Notably, our work shows the incredible DNA exchange potential that chitin-induced *V.*
359 *cholerae* strains exert under co-culture conditions and future studies are therefore required to
360 better understand strain diversity in clinical and environmental settings in the absence of
361 sampling biases.

362

363 **Materials and Methods**

364 **Bacterial strains, plasmids, and growth conditions.** The bacterial strains and plasmids used in
365 this study are described in *SI Appendix*, Table S1. Unless otherwise stated, bacteria were grown
366 aerobically in LB medium under shaking conditions or on solid LB agar plates (1.5% agar).
367 Growth on chitinous surfaces was performed as previously described (27, 48). Additional details
368 are provided in the *SI Appendix*.

369

370 **Preparation of genomic DNA.** Genomic DNA (gDNA) was purified from a 2 ml culture of the
371 respective strain. DNA extraction was performed using 100/G Genomic-tips together with a
372 Genomic DNA buffer set as described in the manufacturer's instructions (Qiagen). After
373 precipitation, the DNA samples were transferred into Tris buffer (10 mM Tris-HCl, pH 8.0). This

374 was preferred over rapid gDNA isolation kits such as the DNeasy Blood & Tissue kit (Qiagen),
375 as the latter isolation kit is strongly biased towards shorter DNA fragments (predominantly 30kb
376 in length compared to up to 150kb for the 100/G columns, as stated by the manufacturer).

377

378 **Natural transformation assay.** Natural transformation assays were performed by adding
379 purified gDNA to the chitin-grown bacteria or by co-culturing the two non-clonal *V. cholerae*
380 strains. To set up the experiments, the bacterial strains were grown as an overnight culture in LB
381 medium at 30°C. After back dilution, the cells were incubated in the presence of chitin flakes
382 (~80 mg; Sigma-Aldrich) submerged in half-concentrated (0.5x) defined artificial seawater
383 medium (11). When purified DNA served as the transforming material, 2 µg of the indicated
384 gDNA was added after 24 h of growth on chitin, and the cells were incubated for another 6 hours.
385 At that point, the bacteria were detached from the chitin surfaces by vigorous vortexing and then
386 were serially diluted. Colony-forming units (CFUs) were enumerated on selective (antibiotic-
387 containing) or non-selective (plain LB) agar plates, and the transformation frequency was
388 calculated by dividing the number of transformants by the total number of CFUs. For mixed
389 community assays, the two strains were inoculated simultaneously at a ratio of 1:1. These
390 mixtures were incubated for 30 h before the bacteria were harvested, diluted, and plated, as
391 described above. All transformation frequency values are averages of three biologically
392 independent experiments except for WGS conditions ② and ④–⑧, wherein the averages of two
393 independent experiments are depicted.

394

395 **Whole-genome sequencing.** For WGS, transformation assays were performed as described
396 above using eight different experimental conditions (Fig. 4 and listed in *SI Appendix*, Table S2).
397 To focus on the acquisition potential of strain A1552, conditions ⑤–⑧ used transformation-
398 deficient prey strains (e.g., Sa5Y derivatives in which a *bla* cassette interrupted the DNA

399 translocation channel protein encoding gene *comEC* (19)). The 360 recovered transformants (3 x
400 20 for experimental conditions ① and ③, which showed high levels of reproducibly, followed by
401 2 x 20 for all other conditions; see *SI Appendix*, Table S2 for details) were grown overnight in
402 LB medium. Genomic DNA extraction was performed as described above. Further processing of
403 the samples was conducted by Microsynth (Balgach, Switzerland). The quality of the DNA
404 samples was verified before DNA libraries were prepared using a Nextera XT Library Prep kit
405 (Illumina). Paired-end sequencing was performed using a NextSeq 500 sequencer (Illumina) with
406 read lengths of 75 nt resulting in mean fragment lengths of around 200 nucleotides.

407

408 **Statistics.** Statistically significant differences were determined by the two-tailed Student's *t*-test
409 where indicated. For natural transformation assays, data were log-transformed (62) before
410 statistical testing. When the number of transformants was below the detection limit, the value
411 was set to the detection limit to allow for statistical analysis.

412

413 **Other methods.** Detailed information on strain design through recombinant DNA techniques
414 and bioinformatic analyses are available in the *SI Appendix* under *Material and Methods*.

415

416 **Data availability.** WGS reads of the 360 transformants have been deposited in NCBI's
417 Sequence Read Archive (SRA) under SRA accession numbers SRR6934824 to SRR6935183
418 according to *SI Appendix*, Table S3. The Bioproject accession number is PRJNA447902.

419

420 **Acknowledgement**

421 The authors thank members of the Blokesch laboratory and F. Le Roux for discussions and A.
422 Boehm for strain Sa5Y. We also acknowledge preliminary bioinformatic analyses by S. Strempel
423 (Microsynth), A.-C. Portmann, and I. Mateus, who also uploaded the sequencing reads to NCBI.

424 This work was supported by EPFL intramural funding, the Swiss National Science Foundation
425 grant 31003A_162551, and a Starting (309064-VIR4ENV) and Consolidator (724630-
426 CholeraIndex) grant from the European Research Council to MB. M.B. is a Howard Hughes
427 Medical Institute (HHMI) International Research Scholar (grant #55008726).

428

429 **Author contributions**

430 N.M. and M.B. designed research; N.M., S.S, C.S, and M.B. performed wetlab experiments; N.G.
431 and C.I. performed bioinformatic analyses; N.M., N.G., C.I., and M.B. discussed the
432 bioinformatic data; M.B. wrote the manuscript with input from N.M., N.G., and C.I. All authors
433 approved the final version.

434

435 The authors declare no conflict of interest.

436

437 **References**

- 438 1. WHO (January 2019) Cholera-Key facts.
- 439 2. Chen I & Dubnau D (2004) DNA uptake during bacterial transformation. *Nat. Rev.*
440 *Microbiol.* 2:241-249.
- 441 3. Johnston C, Martin B, Fichant G, Polard P, & Claverys JP (2014) Bacterial transformation:
442 distribution, shared mechanisms and divergent control. *Nat. Rev. Microbiol.* 12:181-196.
- 443 4. Matthey N & Blokesch M (2016) The DNA-Uptake Process of Naturally Competent *Vibrio*
444 *cholerae*. *Trends Microbiol.* 24:98-110.
- 445 5. Blokesch M & Schoolnik GK (2007) Serogroup conversion of *Vibrio cholerae* in aquatic
446 reservoirs. *PLoS Pathog.* 3:e81.
- 447 6. Croucher NJ, *et al.* (2016) Horizontal DNA Transfer Mechanisms of Bacteria as Weapons of
448 Intragenomic Conflict. *PLoS Biol.* 14:e1002394.

- 449 7. Metzger LC & Blokesch M (2016) Regulation of competence-mediated horizontal gene
450 transfer in the natural habitat of *Vibrio cholerae*. *Curr. Opin. Microbiol.* 30:1-7.
- 451 8. Pruzzo C, Vezzulli L, & Colwell RR (2008) Global impact of *Vibrio cholerae* interactions
452 with chitin. *Environ. Microbiol.* 10:1400-1410.
- 453 9. Gooday GW (1990) Physiology of microbial degradation of chitin and chitosan.
454 *Biodegradation* 1:177-190.
- 455 10. Meibom KL, *et al.* (2004) The *Vibrio cholerae* chitin utilization program. *Proc. Natl. Acad.*
456 *Sci. USA* 101:2524-2529.
- 457 11. Meibom KL, Blokesch M, Dolganov NA, Wu C-Y, & Schoolnik GK (2005) Chitin induces
458 natural competence in *Vibrio cholerae*. *Science* 310:1824-1827.
- 459 12. Li X & Roseman S (2004) The chitinolytic cascade in Vibrios is regulated by chitin
460 oligosaccharides and a two-component chitin catabolic sensor/kinase. *Proc. Natl. Acad. Sci.*
461 *USA* 101:627-631.
- 462 13. Yamamoto S, *et al.* (2014) Regulation of natural competence by the orphan two-component
463 system sensor kinase ChiS involves a non-canonical transmembrane regulator in *Vibrio*
464 *cholerae*. *Mol. Microbiol.* 91:326-347.
- 465 14. Dalia AB, Lazinski DW, & Camilli A (2014) Identification of a membrane-bound
466 transcriptional regulator that links chitin and natural competence in *Vibrio cholerae*. *mBio*
467 5:e01028-13
- 468 15. Yamamoto S, *et al.* (2011) Identification of a chitin-Induced small RNA that regulates
469 translation of the *tfoX* gene, encoding a positive regulator of natural competence in *Vibrio*
470 *cholerae*. *J. Bacteriol.* 193:1953-1965.
- 471 16. Blokesch M & Schoolnik GK (2008) The extracellular nuclease Dns and its role in natural
472 transformation of *Vibrio cholerae*. *J. Bacteriol.* 190:7232-7240.

- 473 17. Lo Scudato M & Blokesch M (2013) A transcriptional regulator linking quorum sensing
474 and chitin induction to render *Vibrio cholerae* naturally transformable. *Nucleic Acids Res.*
475 41:3644-3658.
- 476 18. Jaskólska M, Stutzmann S, Stoudmann C, & Blokesch M (2018) QstR-dependent regulation
477 of natural competence and type VI secretion in *Vibrio cholerae*. *Nucleic Acids Res.*:gky717-
478 gky717.
- 479 19. Seitz P & Blokesch M (2013) DNA-uptake machinery of naturally competent *Vibrio*
480 *cholerae*. *Proc. Natl. Acad. Sci. USA* 110:17987-17992.
- 481 20. Seitz P & Blokesch M (2014) DNA transport across the outer and inner membranes of
482 naturally transformable *Vibrio cholerae* is spatially but not temporally coupled. *mBio*
483 5:e01409-14
- 484 21. Seitz P, *et al.* (2014) ComEA Is Essential for the Transfer of External DNA into the
485 Periplasm in Naturally Transformable *Vibrio cholerae* Cells. *PLoS Genet.* 10:e1004066.
- 486 22. Ellison CK, *et al.* (2018) Retraction of DNA-bound type IV competence pili initiates DNA
487 uptake during natural transformation in *Vibrio cholerae*. *Nature microbiology* 3:773-780.
- 488 23. Adams DW, Stutzmann S, Stoudmann C, & Blokesch M (2018) DNA-uptake pilus of *Vibrio*
489 *cholerae* capable of kin-discriminated auto-aggregation. *bioRxiv doi: 10.1101/354878*
- 490 24. Nielsen KM, Johnsen PJ, Bensasson D, & Daffonchio D (2007) Release and persistence of
491 extracellular DNA in the environment. *Environ. Biosafety Res.* 6:37-53.
- 492 25. Overballe-Petersen S, *et al.* (2013) Bacterial natural transformation by highly fragmented
493 and damaged DNA. *Proc. Natl. Acad. Sci. USA* 110:19860-19865.
- 494 26. Redfield RJ (1988) Evolution of bacterial transformation: is sex with dead cells ever better
495 than no sex at all? *Genetics* 119:213-221.
- 496 27. Borgeaud S, Metzger LC, Scignari T, & Blokesch M (2015) The type VI secretion system
497 of *Vibrio cholerae* fosters horizontal gene transfer. *Science* 347:63-67.

- 498 28. Veening JW & Blokesch M (2017) Interbacterial predation as a strategy for DNA
499 acquisition in naturally competent bacteria. *Nat. Rev. Microbiol.* 15:621-629.
- 500 29. Ho BT, Dong TG, & Mekalanos JJ (2014) A view to a kill: the bacterial type VI secretion
501 system. *Cell host & microbe* 15:9-21.
- 502 30. Galan JE & Waksman G (2018) Protein-Injection Machines in Bacteria. *Cell* 172:1306-1318.
- 503 31. Taylor NMI, van Raaij MJ, & Leiman PG (2018) Contractile injection systems of
504 bacteriophages and related systems. *Mol. Microbiol.* 108:6-15.
- 505 32. Cianfanelli FR, Monlezun L, & Coulthurst SJ (2016) Aim, Load, Fire: The Type VI
506 Secretion System, a Bacterial Nanoweapon. *Trends Microbiol.* 24:51–62.
- 507 33. Metzger LC, *et al.* (2016) Independent Regulation of Type VI Secretion in *Vibrio cholerae*
508 by TfoX and TfoY. *Cell Rep.* 15:951-958.
- 509 34. Jaskólska M & Gerdes K (2015) CRP-dependent positive autoregulation and proteolytic
510 degradation regulate competence activator Sxy of *Escherichia coli*. *Mol Microbiol* 95:833-
511 845.
- 512 35. Metzger LC, Matthey N, Stoudmann C, Collas EJ, & Blokesch M (2019) Ecological
513 implications of gene regulation by TfoX and TfoY among diverse *Vibrio* species.
514 *Environmental microbiology*
- 515 36. Mell JC, Lee JY, Firme M, Sinha S, & Redfield RJ (2014) Extensive cotransformation of
516 natural variation into chromosomes of naturally competent *Haemophilus influenzae*. *G3*
517 4:717-731.
- 518 37. Bubendorfer S, *et al.* (2016) Genome-wide analysis of chromosomal import patterns after
519 natural transformation of *Helicobacter pylori*. *Nature communications* 7:11995.
- 520 38. Alfsnes K, *et al.* (2018) A genomic view of experimental intraspecies and interspecies
521 transformation of a rifampicin-resistance allele into *Neisseria meningitidis*. *Microb. Genom.*

- 523 39. Keymer DP, Miller MC, Schoolnik GK, & Boehm AB (2007) Genomic and phenotypic
524 diversity of coastal *Vibrio cholerae* strains is linked to environmental factors. *Appl. Environ.*
525 *Microbiol.* 73:3705-3714.
- 526 40. Miller MC, Keymer DP, Avelar A, Boehm AB, & Schoolnik GK (2007) Detection and
527 transformation of genome segments that differ within a coastal population of *Vibrio*
528 *cholerae* strains. *Appl. Environ. Microbiol.* 73:3695-3704.
- 529 41. Matthey N, Drebes Dörr NC, & Blokesch M (2018) Long-Read-Based Genome Sequences
530 of Pandemic and Environmental *Vibrio cholerae* Strains. *Microbiol. Resour. Announc.*
531 7:e01574-01518.
- 532 42. Yildiz FH & Schoolnik GK (1998) Role of *rpoS* in stress survival and virulence of *Vibrio*
533 *cholerae*. *J. Bacteriol.* 180:773-784.
- 534 43. Domman D, *et al.* (2017) Integrated view of *Vibrio cholerae* in the Americas. *Science*
535 358:789-793.
- 536 44. Heidelberg JF, *et al.* (2000) DNA sequence of both chromosomes of the cholera pathogen
537 *Vibrio cholerae*. *Nature* 406:477-483.
- 538 45. Dziejman M, *et al.* (2005) Genomic characterization of non-O1, non-O139 *Vibrio cholerae*
539 reveals genes for a type III secretion system. *Proc. Natl. Acad. Sci. USA* 102:3465-3470.
- 540 46. Waldor MK & Mekalanos JJ (1996) Lysogenic conversion by a filamentous phage encoding
541 cholera toxin. *Science* 272:1910-1914.
- 542 47. Mazel D (2006) Integrons: agents of bacterial evolution. *Nat. Rev. Microbiol.* 4:608-620.
- 543 48. Marvig RL & Blokesch M (2010) Natural transformation of *Vibrio cholerae* as a tool-
544 optimizing the procedure. *BMC Microbiol.* 10:155.
- 545 49. Shapiro BJ, *et al.* (2012) Population genomics of early events in the ecological
546 differentiation of bacteria. *Science* 336:48-51.

- 547 50. Mortier-Barriere I, *et al.* (2007) A key presynaptic role in transformation for a widespread
548 bacterial protein: DprA conveys incoming ssDNA to RecA. *Cell* 130:824-836.
- 549 51. Suckow G, Seitz P, & Blokesch M (2011) Quorum sensing contributes to natural
550 transformation of *Vibrio cholerae* in a species-specific manner. *J. Bacteriol.* 193:4914-4924.
- 551 52. Iqbal N, Guerout AM, Krin E, Le Roux F, & Mazel D (2015) Comprehensive Functional
552 Analysis of the 18 *Vibrio cholerae* N16961 Toxin-Antitoxin Systems Substantiates Their
553 Role in Stabilizing the Superintegron. *J. Bacteriol.* 197:2150-2159.
- 554 53. Faruque SM, *et al.* (2004) Genetic diversity and virulence potential of environmental *Vibrio*
555 *cholerae* population in a cholera-endemic area. *Proc. Natl. Acad. Sci. USA* 101:2123-2128.
- 556 54. Mutreja A, *et al.* (2011) Evidence for several waves of global transmission in the seventh
557 cholera pandemic. *Nature* 477:462-465.
- 558 55. Weill FX, *et al.* (2019) Genomic insights into the 2016-2017 cholera epidemic in Yemen.
559 *Nature*
- 560 56. Weill FX, *et al.* (2017) Genomic history of the seventh pandemic of cholera in Africa.
561 *Science* 358:785-789.
- 562 57. Dalia AB, Seed KD, Calderwood SB, & Camilli A (2015) A globally distributed mobile
563 genetic element inhibits natural transformation of *Vibrio cholerae*. *Proc. Natl. Acad. Sci.*
564 *USA* 112:10485-10490.
- 565 58. Blokesch M (2017) In and out-contribution of natural transformation to the shuffling of
566 large genomic regions. *Curr. Opin. Microbiol.* 38:22-29.
- 567 59. Clemens JD, Nair GB, Ahmed T, Qadri F, & Holmgren J (2017) Cholera. *Lancet* 390:1539-
568 1549.
- 569 60. Hang L, *et al.* (2003) Use of *in vivo*-induced antigen technology (IVIAT) to identify genes
570 uniquely expressed during human infection with *Vibrio cholerae*. *Proc. Natl. Acad. Sci. USA*
571 100:8508-8513.

- 572 61. Lombardo MJ, *et al.* (2007) An *in vivo* expression technology screen for *Vibrio cholerae*
573 genes expressed in human volunteers. *Proc. Natl. Acad. Sci. USA* 104:18229-18234.
- 574 62. Keene ON (1995) The log transformation is special. *Stat. Med.* 14:811-819.

575
576
577
578
579
580
581
582
583
584
585
586
587
588
589
590
591
592
593
594
595
596
597
598
599
600
601
602
603
604
605
606
607
608
609

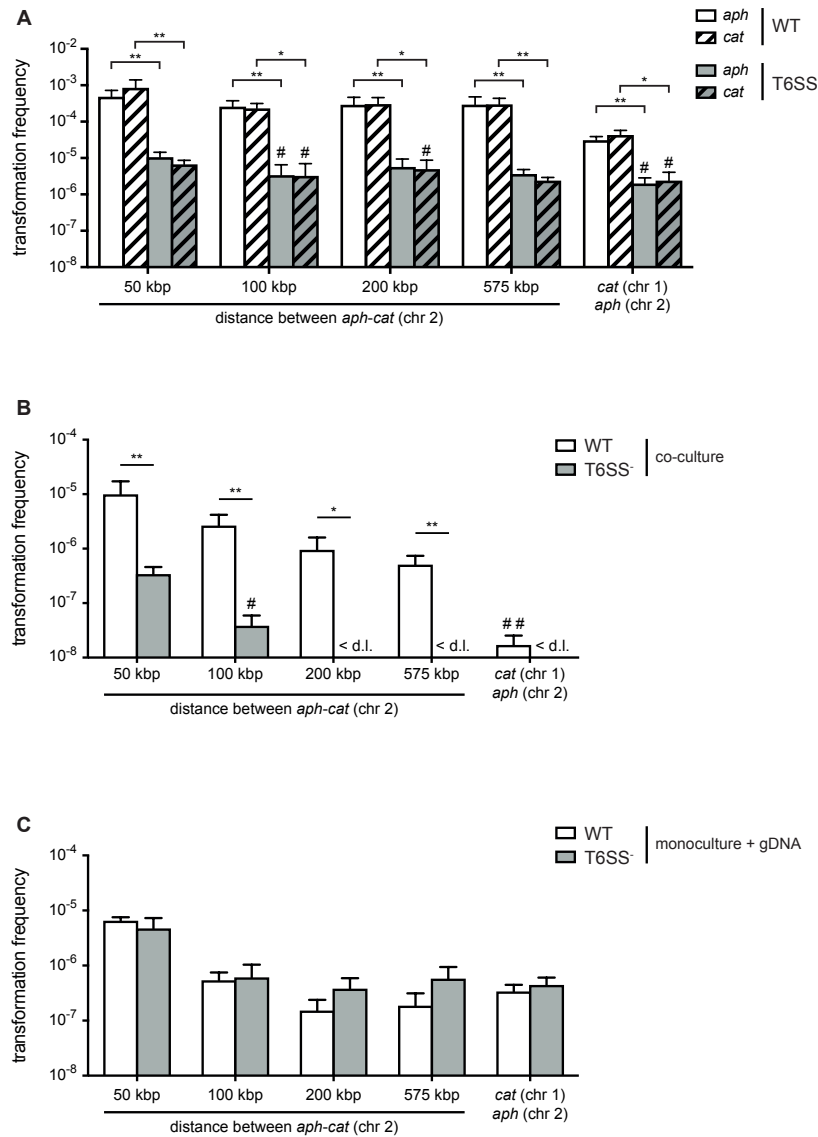


Figure 1: Type VI secretion system (T6SS) enhances horizontal gene transfer (HGT) of single- and double-resistance cassettes if carried *in cis*. (A-B) Transformation occurs in predator/prey co-cultures. To induce natural competence, the WT or a T6SS-negative derivative (A1552Δ*vasK*; T6SS⁻) was co-cultured on chitin with different prey strains (Sa5Y-derived) that carried two antibiotic resistance cassettes: *aph* in *vipA* (chr 2) and *cat* at variable distances from *aph* on the same chromosome or on chr 1, as indicated on the X-axis. Transformation frequencies (Y-axis) indicate the number of transformants that acquired (A) a single resistance cassette or (B) both resistance cassettes divided by the total number of predator colony forming units (CFUs). (C) Natural transformation is not impaired in the T6SS⁻ acceptor strain. Purified genomic DNA (gDNA) was added to competent WT or T6SS⁻ strains. (A-C) Data represent the average of three independent biological experiments (± SD, as depicted by the error bars). For values in which one (#) or two (##) experiments resulted in the absence of transformants, the detection limit was used to calculate the average. <d.l., below detection limit. Statistical significance is indicated (**p* < 0.05; ***p* < 0.01).

610
611
612
613
614
615
616
617
618
619
620
621
622
623
624
625
626
627
628
629
630
631
632
633
634
635
636
637
638
639
640
641
642
643
644
645
646
647
648
649
650
651
652
653
654
655
656
657
658

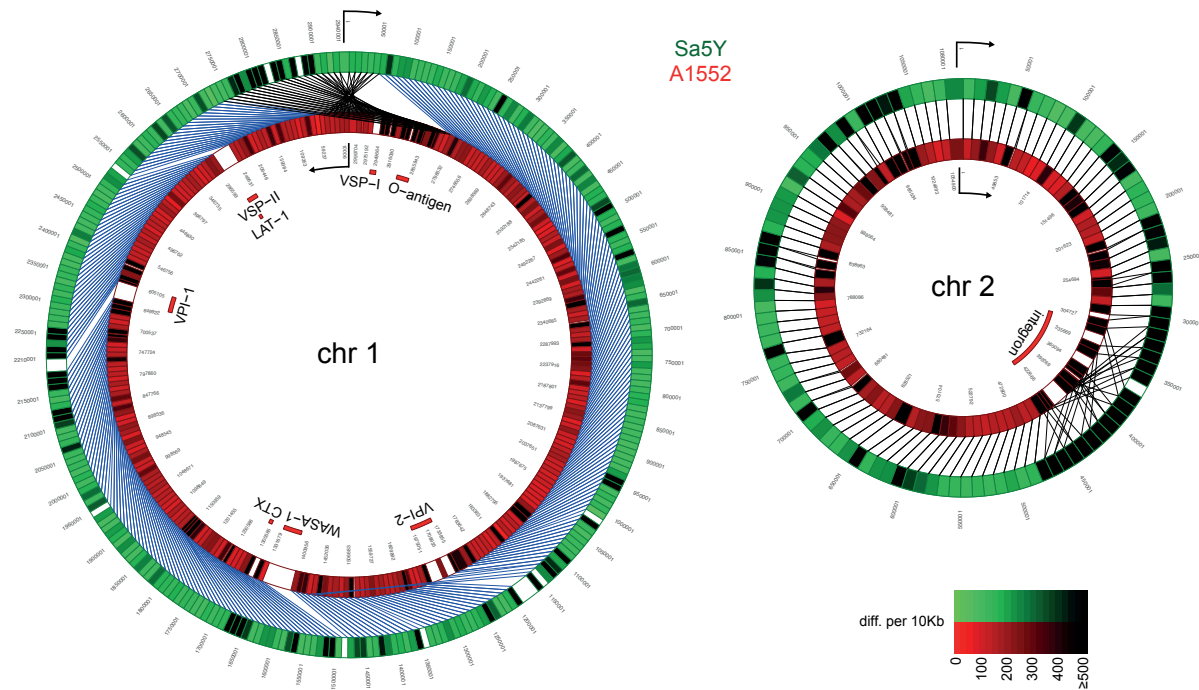


Figure 2: Comparative genomics of pandemic strain A1552 and the environmental isolate Sa5Y. The genomic sequences of chr 1 and 2 of Sa5Y (green) were segmented in 10-kbp-long fragments and aligned against the respective chromosome of the reference A1552 (red). To simplify visualization, chr 1 of strain A1552 was inverted and plotted counter-clockwise relative to Sa5Y (due to the large inversion in this strain; *SI Appendix*), as indicated by the arrow. To represent the differences between the two genomes, a color intensity scale was used that corresponded to the number of differences (SNP or indel), from 0 to ≥ 500 as measured per 10 kbp fragment. White regions show no homology. Important genomic features of pandemic *V. cholerae* are highlighted inside the rings.

659
660
661
662
663
664
665
666
667
668
669
670
671
672
673
674
675
676
677
678
679
680
681
682
683
684
685
686
687
688
689
690
691
692
693
694
695
696
697
698
699
700
701
702

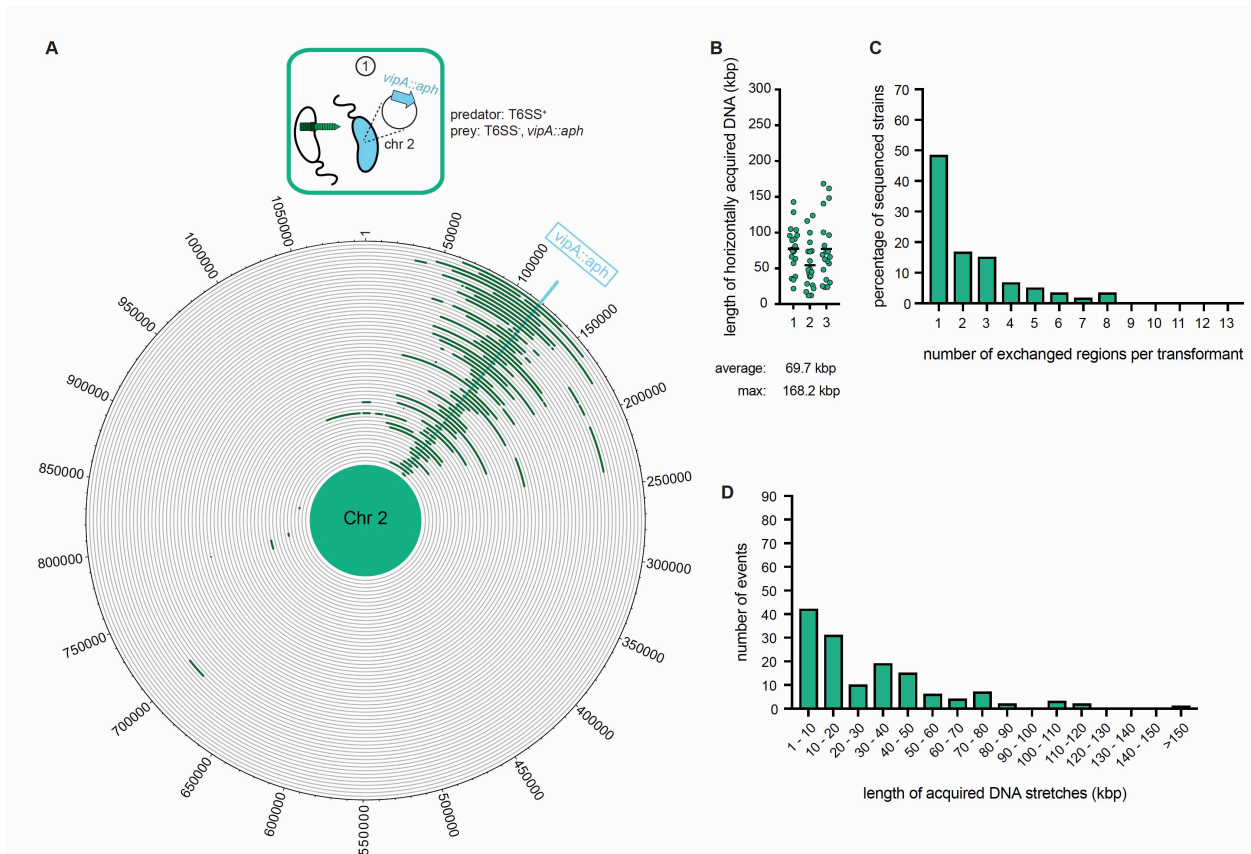
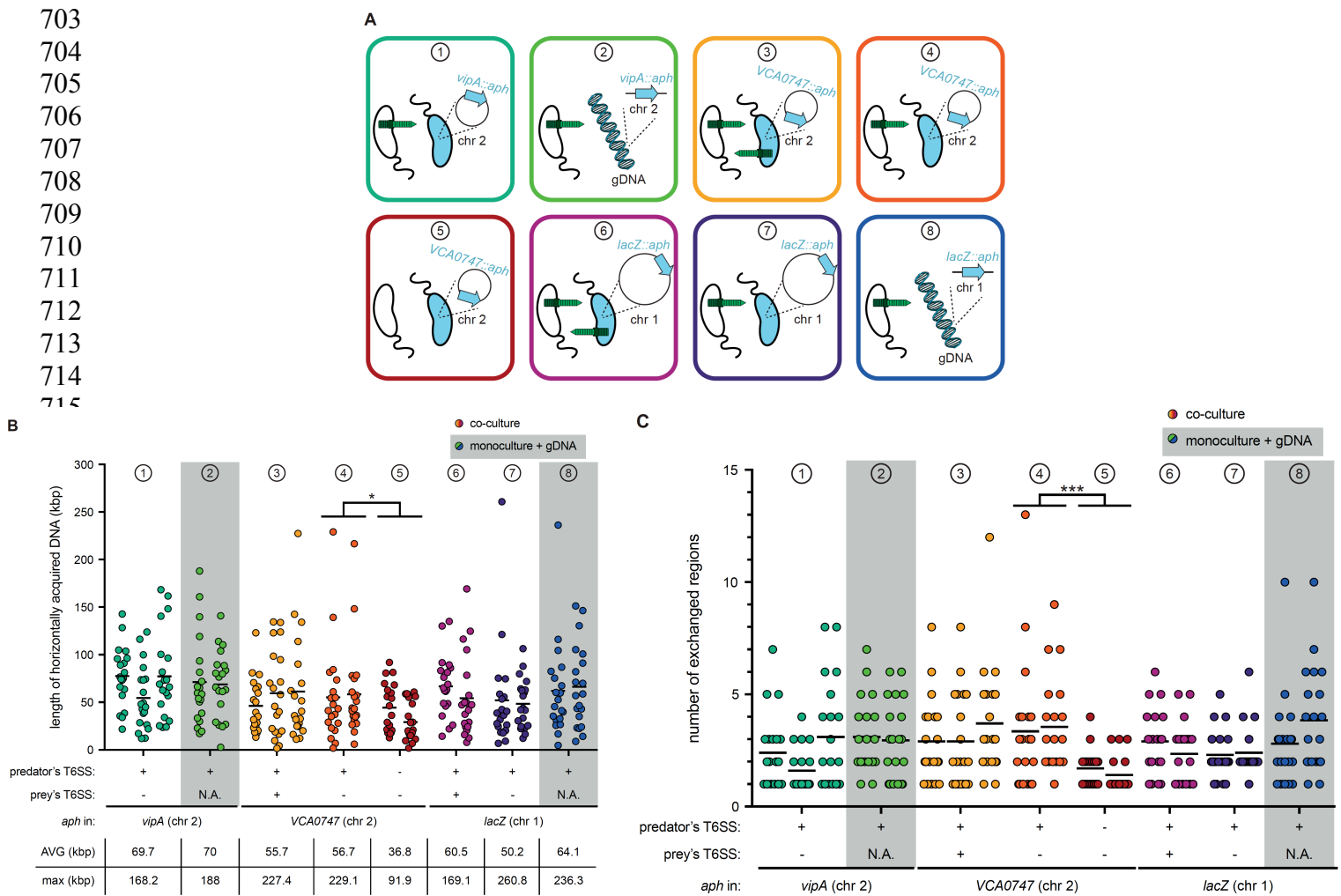


Figure 3: Whole-genome sequencing (WGS)-based quantification of horizontally acquired DNA. WGS analysis of transformants after prey killing and DNA transfer. Twenty kanamycin-resistant transformants were selected per independent biological experiment (n = 3). (A) The scheme represents the experimental setup of the co-culture experiment (condition ①). Sequencing reads for each transformant were mapped onto the prey genomes to visualize the transferred DNA regions (in dark green; see Fig. S4 for both chromosomes). The position of the resistance cassette (*aph*) is indicated by the light blue line. (B) Total DNA acquisition frequently exceeds 100 kb. The total length of horizontally acquired DNA is indicated on the Y-axis for each transformant. Data are from three biologically independent experiments as indicated on the X-axis. Average and maximum lengths are indicated below the graph. (C) Multiple transferred DNA regions were identified in the transformants. Percentage of transformants (n = 60) that exchanged one or more DNA regions, as indicated on the X-axis. (D) Large DNA stretches are transferrable by transformation. The length of individual consecutive DNA stretches was determined as indicated on the X-axis.



734 **Figure 4: T6SS-mediated neighbor predation followed by DNA uptake enhances the**
735 **frequency and length of transferred DNA stretches.** (A) Scheme representing the eight
736 experimental conditions tested in this study. Each scheme indicates whether the transformants
737 acquired the *aph* resistance gene from a prey bacterium (blue) (position of *aph* indicated on the
738 zoomed-in circles of chr 1 or chr 2) or from purified genomic DNA (gDNA). In the former case,
739 the killing capacity of the predator (white) and prey (blue) is shown by the presence or absence
740 of the dark green T6SS structure. The same color code is maintained throughout all figures. (B-C)
741 Transformants from independent biological experiments ($n \geq 2$) were analyzed by WGS for each
742 of the conditions ①-⑧, as indicated at the top of each graph. The main features of predator and
743 prey/gDNA are summarized below the X-axis. Panels (B) and (C) depict the total length of
744 acquired DNA and the number of exchanged DNA stretches, respectively, for each transformant.
745 N.A., not applicable. Statistical analysis is based on a pairwise comparison between different
746 conditions. * $p < 0.05$, *** $p < 0.001$.